Chem Biol Drug Des 2011; **77:** 241–247

Research Article

doi: 10.1111/j.1747-0285.2011.01085.x

N-Substituted Glutamyl Sulfonamides as Inhibitors of Glutamate Carboxypeptidase II (GCP2)

Brian R. Blank[1], Pinar Alayoglu[1], William Engen[1], Joseph K. Choi[2], Clifford E. Berkman[1] and Marc O. Anderson[1]*

[1]*Department of Chemistry and Biochemistry, San Francisco State University, San Francisco, CA 94132, USA*

[2]*Department of Chemistry, Washington State University, Pullman, WA 99164, USA*

**Corresponding author: Marc O. Anderson, marc@sfsu.edu*

Glutamate carboxypeptidase II (GCP2) is a membrane-bound cell-surface peptidase which is implicated in several neurological disorders and is also over-expressed in prostate tumor cells. There is a significant interest in the inhibition of GCP2 as a means of neuroprotection, while GCP2 inhibition as a method to treat prostate cancer remains a topic of further investigation. The key zinc-binding functional group of the well-characterized classes of GCP2 inhibitors (phosphonates and phosphoramidates) is tetrahedral and negatively charged at neutral pH, while glutamyl urea class of inhibitors possesses a planar and neutral zinc-binding group. This study introduces a new class of GCP2 inhibitors, N-substituted glutamyl sulfonamides, which possess a neutral tetrahedral zinc-binding motif. A library containing 15 secondary sulfonamides and 4 tertiary (N-methyl) sulfonamides was prepared and evaluated for inhibitory potency against purified GCP2 enzyme activity. While most inhibitors lacked potency at 100 μM, short alkyl sulfonamides exhibited promising low micromolar potency, with the optimal inhibitor in this series being glutamyl N-(propylsulfonamide) (2g). Lastly, molecular docking was used to develop a model to formulate an explanation for the relative inhibitory potencies employed for this class of inhibitors.

Key words: computational docking, GCP2, glutamate carboxypeptidase II, prostate-specific membrane antigen, PSMA, sulfonamide

Received 21 October 2010, revised 30 December 2010 and accepted for publication 31 December 2010

Neurotoxicity caused by the presence of excess glutamate has been implicated in several neurological disorders including ischemia, traumatic brain injury (TBI), stroke, and amyotrophic lateral sclerosis (ALS) (1–3). By their nature, substances that limit the release of glutamate in the nervous system can be considered neuroprotective agents. One source of glutamate in the nervous system is proteolysis of the short neuropeptide N-acetylaspartylglutamate (NAAG), a reaction catalyzed by the membrane-bound cell-surface peptidase glutamate carboxypeptidase II (GCP2). As such, inhibition of GCP2 causes decreased levels of extracellular glutamate (4), as well as also increased levels of NAAG that itself has a neuroprotective role (5).

GCP2 is also expressed in the human prostate epithelium, and thus, another name for the enzyme is prostate-specific membrane antigen (PSMA) (6). PSMA is over-expressed in prostate cancer tissue and non-prostatic tumor-associated neovasculature (7,8). There are studies suggesting that the inhibition of PSMA by small molecules (2,9) and monoclonal antibodies (2,10,11,12) has potential as therapeutic strategies against prostate cancer. However, the most established use of PSMA inhibitors has been in diagnostic imaging of prostate cancer (1,2,13–21).

There are a number of known classes of GCP2 inhibitor scaffolds, typically characterized by a functional group connected to either a glutaryl moiety or the glutamyl amino group, which either terminates the structure or serves as a linker to another molecular fragment (1,2), (Figure 1). In most inhibitors, glutarate/glutamate appears to occupy the S1' pocket of GCP2 (22,23) while an alternative motif (if present) occupies the S1 pocket. Key classes of inhibitors include the following: phosphonates (**1a**), phosphates (**1b**), phosphoramidates (**1c**-**1e**), and ureas (**1f**) (1,2). In the case of the phosphorous-based inhibitors, the functionalities appear to serve as zinc-binding group (ZBG) to the catalytic zinc atoms in the active site (22,23). A recent structural investigation shows the oxygen in urea-based inhibitors also interact with the catalytic zinc atoms (24). A problem with the highly potent (yet multiply charged) phosphonate inhibitor 2-PMPA (**1a**) is poor oral bioavailability (25) thereby limiting its practical value as a clinical neuroprotective agent.

One goal of our research program is to explore alternative functional groups that could serve as a ZBG group to interact with the catalytically active zinc centers in GCP2. Alternatively, we envision that these functional groups could passively serve as a linker between glutamate and another molecular fragment making favorable contacts in the active site. One attractive scaffold is the glutamyl ureas, which have been explored extensively by Kozikowski *et al.* (2) and have also been co-crystallized with GCP2 (24) Another

functionality is the tetrahedral sulfonamide, because of its trivial installation into small molecule inhibitors. Sulfonamides are attractive for pharmaceutical development, compared to similar phosphorus-based groups (**1a**-**1e**) because of their aqueous stability despite their net neutral charge. One target where sulfonamides have been successfully used as a zinc-binding group is carbonic anhydrase (26–28) Sulfonamide-based inhibitors have also been explored in the context of antiviral and antitumor drug discovery (29–31).

An important feature of sulfonamides (as well as ureas) is the ease in which they can be conjugated to chiral and inexpensive protected glutamate building blocks (**4**) to generate an optically active inhibitor scaffold. In contrast, the highly potent phosphonate inhibitors (e.g., 2-PMPA) are more challenging to produce in optically active form (32).

We envisioned a first generation of simple sulfonamides based on glutamic acid, in which the SAR of various R_1 groups on the sulfur atom could be explored (Figure 2). Two classes of inhibitors were considered: secondary sulfonamides (**2**) and tertiary (N-methyl) sulfonamides (**3**). The latter class of compounds was considered to examine the importance of the free NH group for both inhibitory potency against GCP2 and its potential as a zinc-binding group.

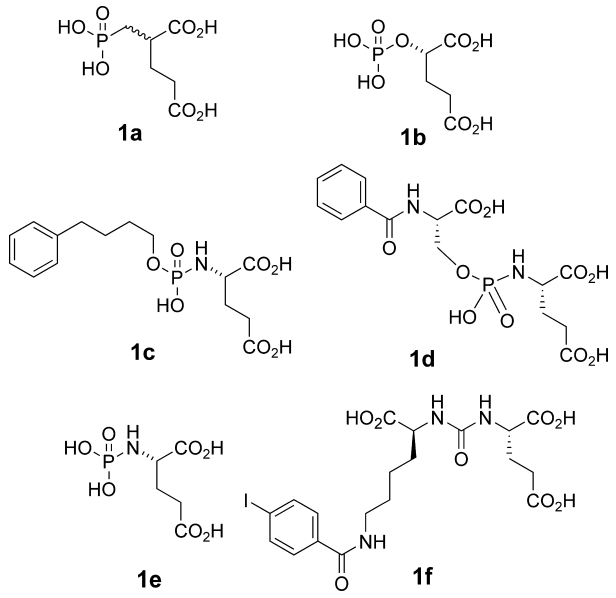

Figure 1: Representative inhibitors of GCP2.

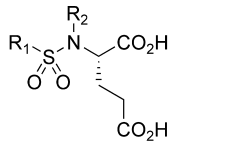

Figure 2: General structure of sulfonamide inhibitors.

Materials and Methods

IC_{50} Determinations for PSMA Inhibition

Inhibition studies were performed as described previously with only minor modifications (33). Working solutions of the substrate (N-[4-(phenylazo)-benzoyl]-glutamyl-g-glutamic acid, PABGgG) and inhibitors were made in TRIS buffer (50 mM, pH 7.4 containing 1% Triton X-100). Working solutions of purified PSMA (50 μg/mL) were diluted in TRIS buffer (50 mM, pH 7.4 containing 1% Triton X-100) to provide from 15% to 20% conversion of substrate to product in the absence of inhibitor. A typical incubation mixture (final volume 250 μL) was prepared by the addition of either 25 μL of an inhibitor solution or 25 μL TRIS buffer (50 mM, pH 7.4 containing 1% Triton X-100) to 175 μL TRIS buffer (50 mM, pH 7.4 containing 1% Triton X-100) in a test tube. PABGgG (25 μL, 100 mM) was added to the above solution. The enzymatic reaction was initiated by the addition of 25 μL of the PSMA working solution. In all cases, the final concentration of PABGgG was 10 mM while the enzyme was incubated with five serially diluted inhibitor concentrations providing a range of inhibition from 10% to 90%. The reaction was allowed to proceed for 15 min with constant shaking at 37 °C and was terminated by the addition of 25 μL methanolic TFA (2% trifluoroacetic acid by volume in methanol) followed by vortexing. The quenched incubation mixture was quickly buffered by the addition of 25 μL K_2HPO_4 (0.1 M), vortexed, and centrifuged (10 min at 7000× *g*). An 85 μL aliquot of the resulting supernatant was subsequently quantified by HPLC as previously described (34,35). IC_{50} values were calculated using KaleidaGraph 3.6 (Synergy Software, Reading, PA, USA).

Synthesis

All solvents used in reactions were both anhydrous and obtained as such from commercial sources. ^1H and ^{13}C NMR spectra were recorded on a Bruker DRX 300 MHz or Bruker Avance 500 MHz spectrometer. ^1H NMR chemical shifts are relative to TMS (δ = 0.00 ppm) or $CDCl_3$ (δ = 7.26 ppm). ^{13}C NMR chemical shifts are relative to $CDCl_3$ (δ = 77.23 ppm). High-resolution mass spectra were obtained by the University of Notre Dame Mass Spectrometry and Proteomics Facility, Notre Dame, IN 46556-5670 using ESI either by direct infusion on a Bruker micrOTOF-II or by LC elution via an ultra-high-pressure Dionex RSLC with C_{18} column coupled with a Bruker micrOTOF-Q II.

General procedure for sulfonamide formation reactions

2-(Ethane-1-sulfonylamino)-pentanedioic acid di-tert-butyl ester (5e)

To a solution of HCl * Glu(OtBu)-OtBu (**4**) (100 mg, 0.338 mmol) in DCM (3.3 mL) was added Et_3N (0.141 mL, 1.014 mmol, 3.0 eq) and ethanesulfonyl chloride (0.034 mL, 0.355 mmol, 1.05 eq). The reaction was stirred 1–2 h, whereupon TLC showed a new spot suspected to be product, and the majority of the amino acid starting

material appeared consumed. The product mixture was dissolved in diethyl ether (25 mL), washed with aq. $NaHCO_3$ (5%) (25 mL), HCl (1 M) (25 mL), and NaCl (satd. aq) (25 mL). The organic layer was dried over Na_2SO_4 and concentrated in vacuo to generate the product (79 mg, 65%) as a colorless oil. ^{1}H NMR (500 mHz, $CDCl_3$) δ 1.37 (t, 3H, J = 7 Hz), 1.43 (s, 9H), 1.48 (s, 9H), 1.84–1.89 (m, 1H), 2.08–2.12 (m, 1H), 2.83–2.41 (m, 2H), 2.98–3.03 (m, 2H), 3.96–4.01 (m, 1H), and 5.07 (d, 1H, J = 9 Hz). ^{13}C NMR (125 mHz, $CDCl_3$) δ 8.8, 28.6, 28.7, 29.2, 31.8, 48.4, 56.6, 81.5, 83.6, 171.9, and 172.6.

General procedure for TFA deprotection reactions

2-Ethenesulfonylamino-pentanedioic acid (2e)

To a solution of 2-ethenesulfonylamino-pentanedioic acid di-tert-butyl ester (**5e**) (0.026 g, 0.076 mmol) was added DCM:TFA (2:1) (0.5 mL). The solution was stirred at RT for 5 h, whereupon TLC showed conversion of starting material to product. Solvent was removed in vacuo to generate the product as a colorless film (0.018 g, 100%). NMR and MS data are shown in Tables S1 and S2.

General procedure for N-methylation reactions

2-[Methyl-(propane-1-sulfonyl)-amino]-pentanedioic acid di-tert-butyl ester (6c)

To a solution of 2-propanesulfonylamino-pentanedioic acid di-tert-butyl ester (**5g**) (15 mg, 0.041 mmol) in DMF (3 mL) was added K_2CO_3 (0.023 g, 0.164 mmol) and 18-crown-6 (11 mg, 0.041 mmol, 1.0 eq), followed by iodomethane (0.010 mL, 0.164 mmol). The solution was heated to 50 °C for 3 h, whereupon TLC showed consumption of starting material and formation of product. The reaction mixture was taken up in ether–ethyl acetate (1:1) (20 mL), washed with H_2O (3 × 20 mL) followed by NaCl (satd. aq.) (20 mL). Subsequently, the organic layer was dried over anhydrous Na_2SO_4, and concentrated in vacuo to provide the product as a colorless oil (11 mg, 73%). ^{1}H NMR (300 mHz, CDCl3) δ 1.04 (t, 3H, J = 7 Hz), 1.45 (s, 9H), 1.47 (s, 9H), 1.83–1.90 (m, 2H), 2.31–2.36 (t, 2H, J = 7 Hz), 2.81 (s, 3H), 2.97–3.04 (m, 2H), and 4.41–4.46 (m, 1H).

2-Azidomethanesulfonylamino-pentanedioic acid di-tert-butyl ester (4f)

To a solution of 2-chloromethanesulfonylamino-pentanedioic acid di-tert-butyl ester (**5c**) (23 mg, 0.062 mmol) in DMF (1 mL) was added sodium azide (16 mg, 0.246 mmol, 4 eq) and 15-crown-5 (0.006 mL, 0.031 mmol, 0.5 eq). The mixture was heated overnight at 100 °C. The reaction mixture was taken up in H_2O (15 mL) and extracted with EtOAc (4 × 20 mL). The organic layer was combined and concentrated in vacuo. The product was isolated after purification by flash column chromatography (4:1 hexanes:ethyl acetate) to yield the product as a colorless oil (15 mg, 66% yield). ^{1}H NMR (300 mHz, $CDCl_3$) δ 1.45 (s, 9H), 1.49 (s, 9H), 1.83–1.93 (m, 1H), 2.08–2.19 (m, 1H), 2.39–2.44 (m, 2H), 4.07–4.11 (m, 1H), 4.25 (d, 1H, J = 15 Hz), 4.34 (d, 1H, J = 15 Hz), and 5.35 (d, 1H, J = 6 Hz). ^{13}C NMR (75 mHz, $CDCl_3$) δ 28.1, 28.3, 28.4, 31.3, 56.8, 67.1, 81.3, 83.5, 170.8, and 172.3.

Results and Discussion

A simple method was employed for the preparation of our library of sulfonamide inhibitors (Scheme 1). Diprotected glutamic acid (**4**) was directly conjugated with commercially available sulfonyl chlorides to generate sulfonamides **5** and deprotected with TFA to the produce the first library of sulfonamide inhibitors **2**. Alternatively, compound **4** was conjugated with sulfonyl chlorides and then treated with iodomethane to generate N-methylsulfonamide analogs **6**, which were deprotected to generate the final N-methylsulfonamide inhibitor library **3**. In general, the purity of the final products, as evidenced by ^{1}H and ^{13}C NMR, was very high (>95%), and the products did not require additional purification. The composition of the library is outlined in Table 1.

Vinyl sulfonamide inhibitor **2e** and methylazido sulfonamide inhibitor **2f** could not be prepared from commercially available sulfonyl chlorides and were synthesized as described in Scheme 2. Thus, protected amino acid **4** was treated with chloroethanesulfonyl chloride to generate intermediate sulfonamide **7**, which underwent elimination *in situ* to generate vinyl sulfonamide **4e**, which was then deprotected as before to **2e**. Likewise, protected chloromethyl sulfonamide **4c** was treated with sodium azide to generate **4f**, which was subsequently deprotected to **2f** (36).

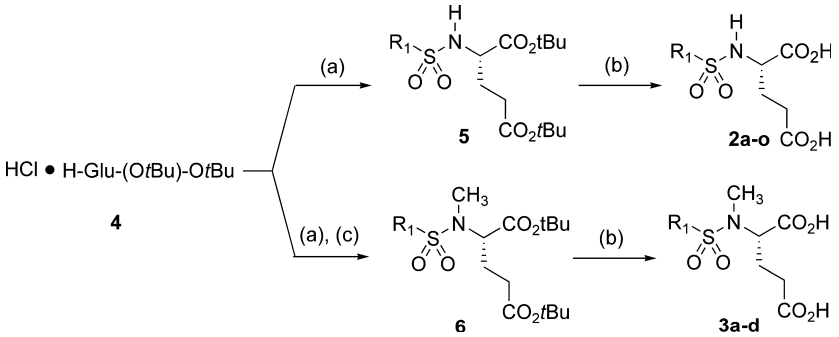

Scheme 1: Synthesis of substituted glutamyl sulfonamides. Reagents and conditions: (a) sulfonyl chloride or triflic anhydride (1.05 eq), Et_3N (3.0 eq), 1h; (b) TFA (20 eq), DCM; (c) CH_3I (4.0 eq), K_2CO_3 (4.0 eq), 16-crown-6 (1.0 eq).

Table 1: Inhibitory potency of sulfonamide derivatives against GCP2 enzymatic activity (IC50 values with error indicated in parenthesis)

Entry	Cmpd	R_1	R_2	% Yield initial sulfonamide formation	% Yield sulfonamide N-methylation	% Yield final deprotection	IC_{50} against purified PSMA μM (error)
1	**2a**	methyl	H	88	n/a	quant	>100
2	**2b**	trifluoromethyl	H	90	n/a	quant	>100
3	**2c**	chloromethyl	H	94	n/a	quant	17.2 (1.5)
4	**2d**	ethyl	H	65	n/a	quant	11.6 (0.4)
5	**2e**	vinyl	H	90[a]	n/a	quant	>100
6	**2f**	methylazido	H	66[b]	n/a	quant	>100
7	**2g**	propyl	H	73	n/a	97	5.0 (0.8)
8	**2h**	butyl	H	98	n/a	95	55.3 (1.9)
9	**2i**	phenyl	H	77	n/a	quant	>100
10	**2j**	4-methylphenyl	H	93	n/a	quant	>100
11	**2k**	2-bromophenyl	H	94	n/a	75	34.0 (2.9)
12	**2L**	2-nitrophenyl	H	94	n/a	85	35.3 (2.2)
13	**2m**	2-pyridyl	H	94	n/a	25	>100
14	**2n**	3-pyridyl	H	60	n/a	30	>100
15	**2o**	2-thiophenyl	H	82	n/a	75	>100
16	**3a**	chloromethyl	CH_3	(above)	82	34	>100
17	**3b**	ethyl	CH_3	(above)	73	quant	>100
18	**3c**	propyl	CH_3	(above)	98	quant	>100
19	**3d**	butyl	CH_3	(above)	65	33	>100

[a]Yield from treatment of 3 with chloroethylsulfonyl chloride to generate vinyl sulfonamide **4e**

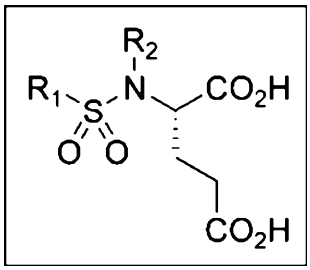

(Scheme 2).

[b]Yield from treatment of **5c** with sodium azide/DMF to generate methylazido sulfonamide **4f** (Scheme 2).

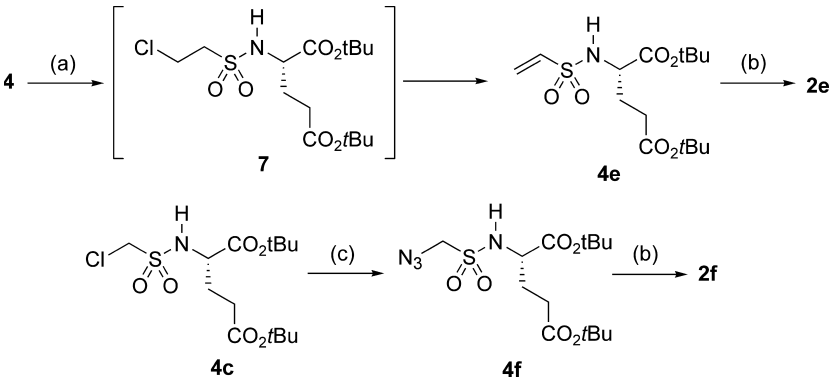

Scheme 2: Synthesis of sulfonamides **2e** and **2f**. Reagents and conditions: (a) 2-chloroethanesulfonyl chloride (1.4 eq), Et_3N (2.5 eq); (b) TFA (20 eq), DCM; (c) NaN_3 (4.0 eq), 15-crown-5 (0.5 eq), DMF, overnight, 95 °C.

Using the methodology described in Scheme 1, a library of inhibitor candidates was prepared, to explore a variety of simple alkyl (**2a**-**2d**, **2f**-**2h**), vinyl (**2e**) and aryl (**2i**-**2L**) fragments at the R_1 position and also to explore the effect of incorporating an N-methyl substituent into the sulfonamide inhibitor structure (**3a**-**3d**) (Table 1). In addition to substituted aromatic rings, three heteroaromatic ring systems were also evaluated: **2m-2o**, with the rational that at least **2m** and **2o** contain hydrogen bond acceptor atoms (N and S) which could potentially enhance zinc-binding with GCP2.

Once prepared, the sulfonamide inhibitors **2a**-**2o** and **3a-3d** were assayed for inhibition against purified GPC2 using conditions that were described previously (33) with results indicated as 50% inhibitory (IC_{50}) values. The majority of the compounds screened were inactive at 100 μM. However, we found that several small alkyl inhibitors in compound series **2** possessed measurable potency, including the chloromethyl (**2c**), ethyl (**2d**), and propyl (**2g**) sulfonamides, with the latter inhibitor being the most potent in this series. The butyl homolog (**2h**) obtained relatively weak potency (55 μM) but was still more potent than the majority of the inactive inhibitors that lacked notable potency at 100 μM. Overall, comparing the short N-alkyl sulfonamide inhibitors, it appears that propyl (**2g**) has the optimal carbon chain length (IC_{50} 5 μM). The ethyl (**2d**) and bioisosteric chloromethyl (**2c**) sulfonamide obtained reduced potency (IC_{50} 11.6 and 17.2 μM, respectively) while methyl and trifluoromethyl sulfonamides were inactive. In terms of aromatic sulfonamides, the 2-bromophenyl (**2k**) and 2-nitrophenyl (**2L**) sulfonamides were more potent than others in this class, but could not compete with the short alkyl sulfonamide inhibitors. The heteroaromatic sulfonamide inhibitors (**2m**-**2o**) appeared to be devoid of potency.

To establish a tentative mode of binding of the most potent set of inhibitors, computational docking was employed. As such, the entire set of sulfonamides (**2a**-**2o** and **3a**-**3f**) was docked into a high-resolution X-ray crystal structure (PDB = 2C6C) (37), which was co-crystallized with the potent phosphonate inhibitor GPI-18431 (Figure 3). Additionally, the compounds were docked into a different crystal structure (PDB = 3D7H) (24), which was co-crystallized with the urea inhibitor DCIBzL. Docking of each inhibitor was performed with FRED2 (OpenEyes) employing a library of ligand conformations generated by OMEGA (OpenEyes) with protonation states determined by the small molecule ionization tool implemented in PIPELINE PILOT (Accelrys).

Upon docking this series of inhibitors, several observations were made as follows:

(1) the N-(alkylsulfonamide) inhibitors do not adopt the binding mode of the other well-characterized inhibitor classes (phosphonate, phosphoramidate, urea, etc.), in which the glutamate clearly fits in the S1'-binding pocket making connections to Lys^{699} and Asn^{257} (gamma-carboxyl), and Arg^{210} (alpha-carboxyl) (Figure 3A). This was concluded by examining not only at the lowest energy binding mode of the inhibitors, but an entire selection of 20 alternate poses for the alkyl inhibitors. The steric features simply exclude this possibility for the alkyl sulfonamide inhibitors, as well as the aromatic and N-methyl inhibitors.

(2) The binding mode of the alkyl sulfonamide inhibitors appears 'backward', in which the glutamate and R group on the sulfonamide are configured oppositely when compared to the conventional mode. Notably, there are known inhibitors that lack a glutamate residue, indicating that filling the S1' pocket with glutamate is not necessary for binding (23,38). The new binding mode was observed consistently with a series of alkyl sulfonamide compounds, docking into two different X-ray crystal structures (2G6C and 3D7H).

(3) The feature we observe with our most potent inhibitor (propyl, **2g**, IC_{50} = 5 μM) is the near filling of a cavity flanked by Asn^{257} and Lys^{699} (Figure 3C). The less potent ethyl analog (**2d**) (IC_{50} = 10 μM) (Figure 3B) and chloromethyl analog (IC_{50} = 17.2 μM) fill this cavity less completely. In these three molecules (among

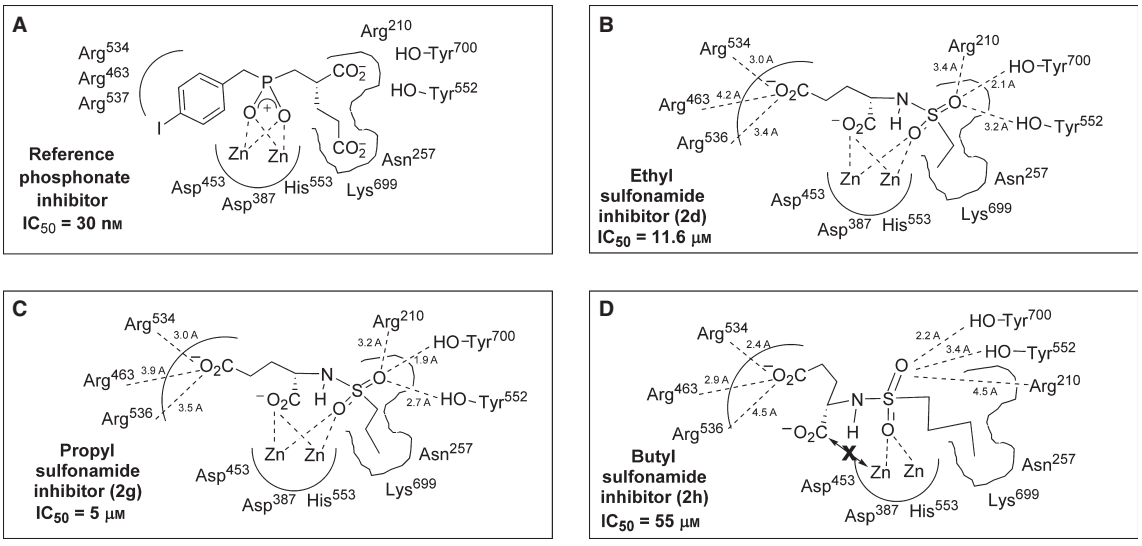

Figure 3: Binding mode of sulfonamide GCP2 inhibitors. (A) conventional mode of binding for phosphonates, phosphoramidates, ureas determined by X-ray crystallography, as demonstrated by inhibitor GPI-18431 (PDB = 2C6C) (B) tentative binding mode for alkyl sulfonamide inhibitors, in this case the ethyl sulfonamide (**2d**), which has limited hydrophobic contacts with the cavity flanked by Lys^{699} and Asn^{257}; (C) tentative binding model for propyl sulfonamide (**2g**), which fills the Asn^{257} and Lys^{699} cavity more completely, possibly explaining its improved potency; (D) tentative binding mode for the butyl sulfonamide inhibitor (**2h**), which has relatively low potency (IC_{50} = 55 μM), possibly explained by the extra alkyl CH_2 group forcing the α-carboxyl away from GCP2 zinc atoms, eliminating this key proposed interaction. For 3D representations of docked small molecule inhibitors, see Supporting Information (Figures S1-S3).

other small alkyl sulfonamides), a key interaction occurs between the glutamate α-carboxyl and the catalytic zinc atoms. One sulfonamide oxygen atom makes an additional putative interaction with zinc, while the other oxygen interacts with Arg^{210}, and the phenols of Tyr^{700} and Tyr^{552}.

The relatively poor butyl sulfonamide inhibitor (IC_{50} = 55 μM) does not fit well into this cavity, because of its size, creating a steric clash (Figure 3D). The clash is resolved by forcing the alpha-carboxyl group away from the GCP2 catalytic zinc atoms, destroying a potentially valuable interaction. This most likely costs the inhibitor in a significant drop in potency.

(4) The N-methyl inhibitors generally dock in an orientation preventing the key interactions from occurring (particularly between the α-carboxyl group and the zinc atoms), and their inactivity is not surprising. The aromatic sulfonamides also adopt a different binding mode, closer to the conventional inhibitor binding mode, although they are still unable to make the key γ-carboxyl interactions with Asn^{257}, Lys^{699} that the conventional inhibitors make (data not shown).

Conclusion and Future Directions

A small library of N-substituted glutamyl sulfonamide inhibitors of GCP2 was prepared. Inhibition data were determined for the series of compounds. While the majority of the inhibitors were inactive, a small collection of inhibitors containing short alkyl sulfonamide substituents possessed low micromolar activity, with the best compound being the propyl sulfonamide (**2g**). The relative potencies were rationalized by a model generated through computational docking. Namely, the most potent compound (**2g**) optimally filled a pocket flanked by the residues Asn^{257} and Lys^{699}. We suggest that sulfonamides that contained fewer or more or more carbon atoms were unable to fill this cavity and in turn achieved reduced potency. Based on the SAR model determined by modeling, we plan to generate additional compounds that we expect will obtain improved electrostatic interactions (particularly with Lys^{699}), and these results will be reported in due course.

Acknowledgements

This work was supported in part by grants from the National Institutes of Health (SC2 GM-084867-01 A1 and 1R01CA140617-01A2). Brian Blank acknowledges a fellowship funded by the Arnold and Mabel Beckman Foundation. Mass spectrometry services at University of Notre Dame were supported by grants from the National Science Foundation (CHE-0741793). Lastly, the authors acknowledge OpenEyes Inc. and Accelrys Inc. for providing free site licenses to the academic community.

References

1. Tsukamoto T., Wozniak K.M., Slusher B.S. (2007) Progress in the discovery and development of glutamate carboxypeptidase II inhibitors. Drug Discov Today;12:767–776.
2. Zhou J., Neale J.H., Pomper M.G., Kozikowski A.P. (2005) NAAG peptidase inhibitors and their potential for diagnosis and therapy. Nat Rev Drug Discov;4:1015–1026.
3. Whelan J. (2000) NAALADase inhibitors: A novel approach to glutamate regulation. Drug Discov Today;5:171–172.
4. Vornov J.J., Wozniak K., Lu M., Jackson P., Tsukamoto T., Wang E., Slusher B. (1999) Blockade of NAALADase: a novel neuroprotective strategy based on limiting glutamate and elevating NAAG. Ann N Y Acad Sci;890:400–405.
5. Kamiya H., Shinozaki H., Yamamoto C. (1996) Activation of metabotropic glutamate receptor type 2/3 suppresses transmission at rat hippocampal mossy fibre synapses. J Physiol;493 (Pt 2):447–455.
6. Carter R.E., Feldman A.R., Coyle J.T. (1996) Prostate-specific membrane antigen is a hydrolase with substrate and pharmacologic characteristics of a neuropeptidase. Proc Natl Acad Sci U S A;93:749–753.
7. Haffner M.C., Kronberger I.E., Ross J.S., Sheehan C.E., Zitt M., Muhlmann G., Ofner D., Zelger B., Ensinger C., Yang X.J., Geley S., Margreiter R., Bander N.H. (2009) Prostate-specific membrane antigen expression in the neovasculature of gastric and colorectal cancers. Hum Pathol;40:1754–1761.
8. Chang S.S., O'Keefe D.S., Bacich D.J., Reuter V.E., Heston W.D., Gaudin P.B. (1999) Prostate-specific membrane antigen is produced in tumor-associated neovasculature. Clin Cancer Res;5(10): 2674–2681.
9. Tang H., Brown M., Ye Y., Huang G., Zhang Y., Wang Y., Zhai H., Chen X., Shen T.Y., Tenniswood M. (2003) Prostate targeting ligands based on N-acetylated alpha-linked acidic dipeptidase. Biochem Biophys Res Commun;307:8–14.
10. Chang S.S. (2004) Monoclonal antibodies and prostate-specific membrane antigen. Curr Opin Investig Drugs;5:611–615.
11. Chang S.S. (2004) Overview of prostate-specific membrane antigen. Rev Urol;6(Suppl 10):S13–S18.
12. Elsasser-Beile U., Buhler P., Wolf P. (2009) Targeted therapies for prostate cancer against the prostate specific membrane antigen. Curr Drug Targets;10:118–125.
13. Bander N.H., Milowsky M.I., Nanus D.M., Kostakoglu L., Vallabhajosula S., Goldsmith S.J. (2005) Phase I trial of 177lutetium-labeled J591, a monoclonal antibody to prostate-specific membrane antigen, in patients with androgen-independent prostate cancer. J Clin Oncol;23:4591–4601.
14. Foss C.A., Mease R.C., Fan H., Wang Y., Ravert H.T., Dannals R.F., Olszewski R.T., Heston W.D., Kozikowski A.P., Pomper M.G., Johns Hopkins University, B. M. U. S. A. (2005) Radiolabeled small-molecule ligands for prostate-specific membrane antigen: in vivo imaging in experimental models of prostate cancer. Clin Cancer Res;11:4022–4028.
15. Pomper M.G., Musachio J.L., Zhang J., Scheffel U., Zhou Y., Hilton J., Maini A., Dannals R.F., Wong D.F., Kozikowski A.P. (2002) 11C-MCG: synthesis, uptake selectivity, and primate PET of a probe for glutamate carboxypeptidase II (NAALADase). Mol Imaging;1:96–101.
16. Guilarte T.R., McGlothan J.L., Foss C.A., Zhou J., Heston W.D., Kozikowski A.P., Pomper M.G., Department of Environmental Health Sciences, J. H. S. o. P. H. B. M. D. U. S. A. (2005) Glutamate carboxypeptidase II levels in rodent brain using [125I]DCIT quantitative autoradiography. Neurosci Lett;387(3):141–144.

17. Humblet V., Lapidus R., Williams L.R., Tsukamoto T., Rojas C., Majer P., Hin B., Ohnishi S., De Grand A.M., Zaheer A., Renze J.T., Nakayama A., Slusher B.S., Frangioni J.V. (2005) High-affinity near-infrared fluorescent small-molecule contrast agents for in vivo imaging of prostate-specific membrane antigen. Mol Imaging;4:448–462.
18. Banerjee S.R., Foss C.A., Castanares M., Mease R.C., Byun Y., Fox J.J., Hilton J., Lupold S.E., Kozikowski A.P., Pomper M.G. (2008) Synthesis and evaluation of technetium-99m- and rhenium-labeled inhibitors of the prostate-specific membrane antigen (PSMA). J Med Chem;51:4504–4517.
19. Mease R.C., Dusich C.L., Foss C.A., Ravert H.T., Dannals R.F., Seidel J., Prideaux A., Fox J.J., Sgouros G., Kozikowski A.P., Pomper M.G. (2008) N-[N-[(S)-1,3-Dicarboxypropyl]carbamoyl]-4-[18F]fluorobenzyl-L-cysteine, [18F]DCFBC: a new imaging probe for prostate cancer. Clin Cancer Res;14:3036–3043.
20. Lapi S.E., Wahnishe H., Pham D., Wu L.Y., Nedrow-Byers J.R., Liu T., Vejdani K., VanBrocklin H.F., Berkman C.E., Jones E.F. (2009) Assessment of an 18F-labeled phosphoramidate peptidomimetic as a new prostate-specific membrane antigen-targeted imaging agent for prostate cancer. J Nucl Med;50:2042–2048.
21. Dijkgraaf I., Boerman O.C. (2009) Radionuclide imaging of tumor angiogenesis. Cancer Biother Radiopharm;24:637–647.
22. Barinka C., Rovenska M., Mlcochova P., Hlouchova K., Plechanovova A., Majer P., Tsukamoto T., Slusher B.S., Konvalinka J., Lubkowski J. (2007) Structural insight into the pharmacophore pocket of human glutamate carboxypeptidase. J Med Chem;50:3267–3273.
23. Mesters J.R., Henning K., Hilgenfeld R. (2007) Human glutamate carboxypeptidase II inhibition: structures of GCPII in complex with two potent inhibitors, quisqualate and 2-PMPA. Acta Crystallogr D Biol Crystallogr;63:508–513.
24. Barinka C., Byun Y., Dusich C.L., Banerjee S.R., Chen Y., Castanares M., Kozikowski A.P., Mease R.C., Pomper M.G., Lubkowski J. (2008) Interactions between human glutamate carboxypeptidase II and urea-based inhibitors: structural characterization. J Med Chem;51:7737–7743.
25. Peng X.Q., Li J., Gardner E.L., Ashby C.R. Jr, Thomas A., Wozniak K., Slusher B.S., Xi Z.X. (2010) Oral administration of the NAALADase inhibitor GPI-5693 attenuates cocaine-induced reinstatement of drug-seeking behavior in rats. Eur J Pharmacol;627:156–161.
26. Bonnac L., Innocenti A., Winum J.-Y., Casini A., Montero J.-L., Scozzafava A., Barragan V., Supuran C.T. (2004) Carbonic anhydrase inhibitors. Sulfonamide diuretics revisited–old leads for new applications? J Enzyme Inhib Med Chem;pp. 275–278.
27. Temperini C., Cecchi A., Scozzafava A., Supuran C.T. (2008) Carbonic anhydrase inhibitors. Sulfonamide diuretics revisited–old leads for new applications? Org Biomol Chem;6:2499–2506.
28. Supuran C.T. (2008) Carbonic anhydrases: novel therapeutic applications for inhibitors and activators. Nat Rev Drug Discov;7:168–181.
29. Scozzafava A., Owa T., Mastrolorenzo A., Supuran C.T. (2003) Anticancer and antiviral sulfonamides. Curr Med Chem;10:925–953.
30. Supuran C.T., Casini A., Scozzafava A. (2003) Protease inhibitors of the sulfonamide type: anticancer, antiinflammatory, and antiviral agents. Med Res Rev;23:535–558.
31. Supuran C.T., Innocenti A., Mastrolorenzo A., Scozzafava A. (2004) Antiviral sulfonamide derivatives. Mini Rev Med Chem;4:189–200.
32. Vitharana D., France J.E., Scarpetti D., Bonneville G.W., Majer P., Tsukamoto T. (2002) Synthesis and biological evaluation of (R)- and (S)-2-(phosphonomethyl)pentanedioic acids as inhibitors of glutamate carboxypeptidase II. Tetrahedron Asymmetry;13:1609–1614.
33. Wu L.Y., Anderson M.O., Toriyabe Y., Maung J., Campbell T.Y., Tajon C., Kazak M., Moser J., Berkman C.E. (2007) The molecular pruning of a phosphoramidate peptidomimetic inhibitor of prostate-specific membrane antigen. Bioorg Med Chem;15:7434–7443.
34. Maung J., Mallari J.P., Girtsman T.A., Wu L.Y., Rowley J.A., Santiago N.M., Brunelle A.N., Berkman C.E. (2004) Probing for a hydrophobic a binding register in prostate-specific membrane antigen with phenylalkylphosphonamidates. Bioorg Med Chem; 12:4969–4979.
35. Anderson M.O., Wu L.Y., Santiago N.M., Moser J.M., Rowley J.A., Bolstad E.S., Berkman C.E. (2007) Substrate specificity of prostate-specific membrane antigen. Bioorg Med Chem;15:6678–6686.
36. Zhou A., Rayabarapu D., Hanson P.R. (2008) Click, Click, Cyclize: A DOS Approach to Sultams Utilizing Vinyl Sulfonamide Linchpins. Organic Letters;11:531–534.
37. Mesters J.R., Barinka C., Li W., Tsukamoto T., Majer P., Slusher B.S., Konvalinka J., Hilgenfeld R. (2006) Structure of glutamate carboxypeptidase II, a drug target in neuronal damage and prostate cancer. EMBO J;25:1375–1384.
38. Wang H., Byun Y., Barinka C., Pullambhatla M., Bhang H.E., Fox J.J., Lubkowski J., Mease R.C., Pomper M.G. (2010) Bioisosterism of urea-based GCPII inhibitors: Synthesis and structure-activity relationship studies. Bioorg Med Chem Lett;20:392–397.

Supporting Information

Additional Supporting Information may be found in the online version of this article:

Figure S1. Three-dimensional pose of ethyl sulfonamide inhibitor **2d** (11.6 μM) docked into the active site of GCP2 (PDB = 2C6C).

Figure S2. Three-dimensional pose of propyl sulfonamide inhibitor **2g** (5 μM, most potent in this series) docked into the active site of GCP2 (PDB = 2C6C).

Figure S3. Three-dimensional pose of butyl sulfonamide inhibitor **2h** docked into the active site of GCP2 (PDB = 2C6C). The n-butyl group forces the glutamate α-carboxyl group away from the catalytic zinc atoms, producing a significant drop in potency (55 μM).

Table S1. Characterization of sulfonamide products by 1H NMR and MS (low res or high res).

Table S2. Characterization of representative sulfonamide products (**2**) and protected intermediates (**4**, **5**) by ^{13}C NMR.

Please note: Wiley-Blackwell is not responsible for the content or functionality of any supporting materials supplied by the authors. Any queries (other than missing material) should be directed to the corresponding author for the article.